An Advanced Technique for Measuring the Effect of Moisture Content on the Thermal Conductivity of Fumed Silica VIPs and the Equilibrium Water Vapor Pressure of Desiccants

Introduction

The degradation rate of VIPs depends not only on the permeation rate of the different atmospheric gases through the envelope, but also on the response of the core material to the increasing presence of these permeated gas molecules. Field tests on fumed silica (FS) panels show that the degradation rate of FS panels is predominantly determined by the moisture permeating through the envelope, and much less by the permeating air molecules. Over the last few years Avery Dennison Hanita has developed a very efficient and easy-to-operate technique for measuring the response of any core material to the increasing pressure of air (λ vs P). However, there is no easy-to-operate technique available for measuring the relationship between the amount of moisture absorbed by FS cores and their thermal conductivity. In this project, Avery Dennison Hanita faced this challenge by upgrading and modifying the λ vs P technology to apply it to moisture content (MC), the λ vs MC curve. In addition to λ vs MC, the upgraded technology may be applied to investigate the adsorption capabilities of several desiccants which are commonly used with glass fiber cores.

This newly developed technique can be used by laboratories for qualification of commercial panels, and by both labs and industrial companies to characterize newly developed core materials.

Background

Accurate prediction of the long-term performance of panels is very important for creating reliable industrial standards for VIPs. It is also a significant factor in the development of new core materials, since the response to accumulated moisture has a huge effect on performance throughout their decades-long service life.

In the early 21st century, pioneering experimental work was made (1) to measure the dependence of the thermal conductivity of fumed silica samples by exposing the core to different levels of moisture, re-evacuating the panel and measuring its thermal conductivity by the guarded hot plate technique. The internal moisture vapor pressure was measured using the liftoff technique. Two of the most important results of the ZAE work are presented below. Figure 1 shows how the thermal conductivity of a 20mm thick fumed silica panel changes with moisture content levels at a mean temperature of 10°C. The second figure presents the relationship between the moisture content and the relative humidity inside the panel - the sorption isotherms curves.

Figure 1

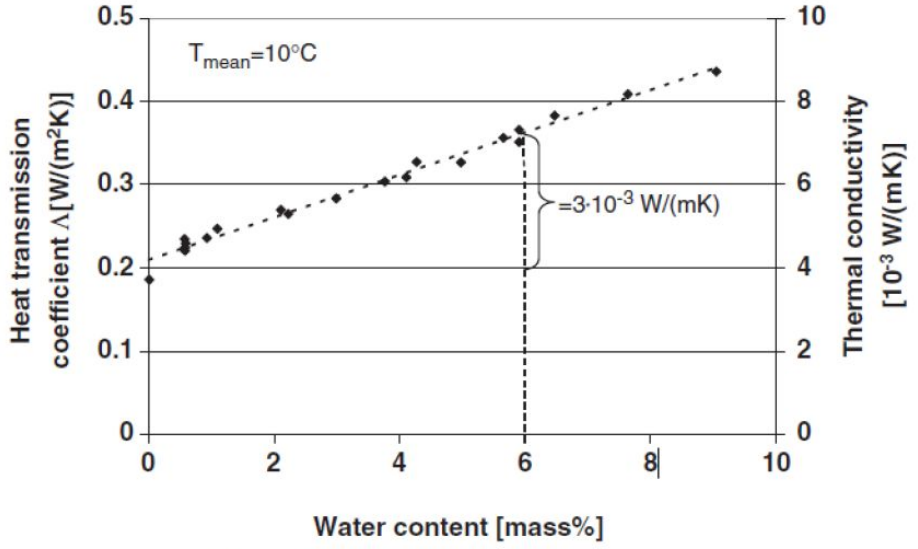

Heat transmission coefficient Λ (left) and thermal conductivity λ (right) depending on the water content X_w in 20-mm thick VIPs at a mean temperature of 10°C.

Figure 2

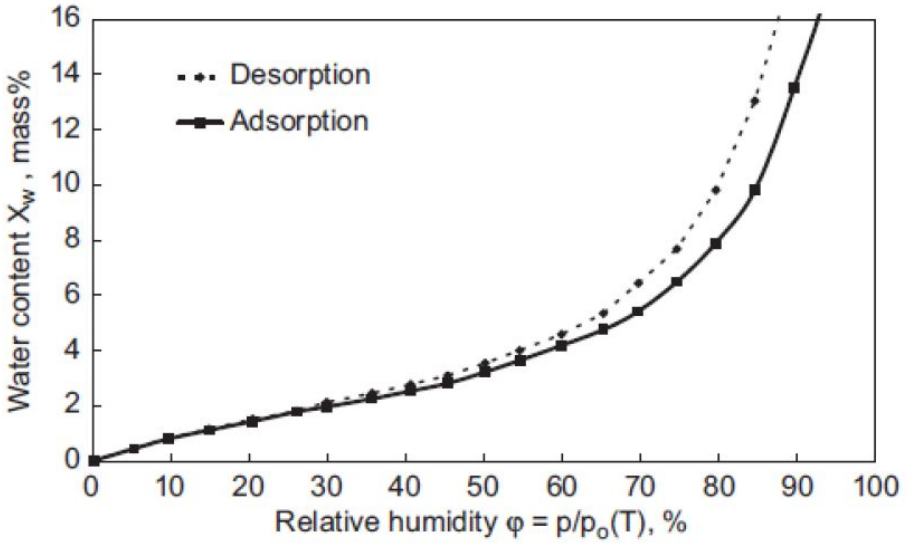

Sorption isotherms for fumed silica kernels at 23 °C. Plotted is the water content in mass% of the dry kernel versus the relative vapour pressure [20].

This report describes a new generation of measuring techniques that allows easier and faster procedures. In addition, no extra pressure measurement by the liftoff device is required. In the new technique, both the thermal conductivity and the pressure of the moisture vapor are measured simultaneously by a very accurate pressure gauge connected to the internal volume of the panels. During the project, the new measuring technique was applied to four types of fumed silica cores and three desiccants, providing a new understanding of the effect of moisture absorption on the thermal conductivity of the fumed silica cores and adsorption capabilities of several desiccants.

Description of Measuring Technique

The newly proposed approach is based on the successful technique developed by Avery Dennison Hanita for measuring the λ vs P curves of core materials, as shown in Figure 3 below. The core under testing is located at the left side of the envelope while a leak-tight connector is mounted on the right side of the bag. The flat left side is used for measuring the thermal conductivity of the core while the connector on the right is used for evacuating the panel, accurately measuring the internal pressure using two pressure gauges and for delivering controlled and accurately measured portions of water into the evacuated volume of the tested panel.

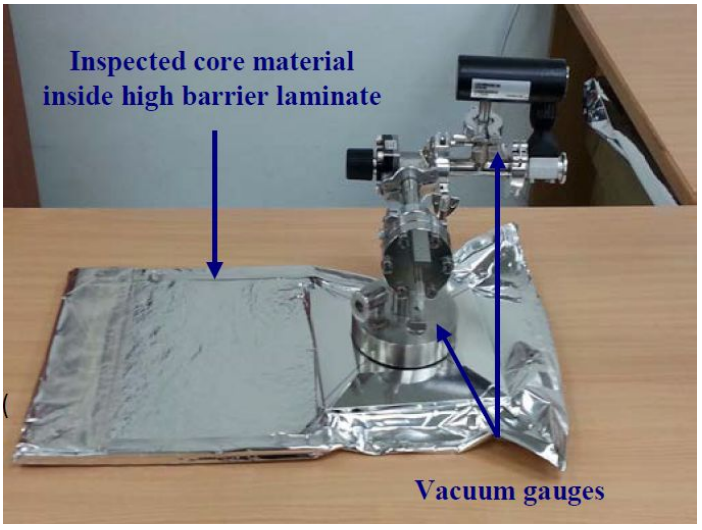

Figure 3: Picture of the system for core materials characterization (λ vs P curve)

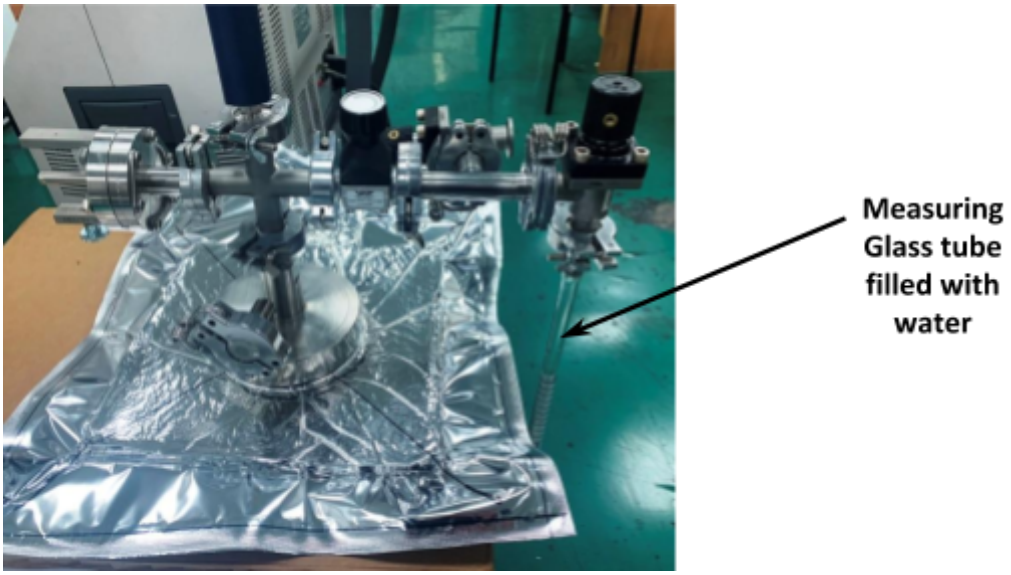

Figure 4: The system for determining the λ vs MC curves

A water measuring tube is connected to the vacuum valve which previously was used for evacuating the panel. This allows a measured quantity of moisture through a vacuum valve into the evacuated space (fumed silica core or desiccant).

Equipment used

a. LaserComp 314 heat flux λ machine
b. Vacuum gauges – Capacitive (10 mbar full range) and SRG (spinning rotor gauge)
c. Turbo molecular pump

Samples tested:

a. Four types of fumed silica blocks were tested:
    1. Core A - Hydrophobic
    2. Core B - Hydrophilic - surface area (BET) 200 g/m^2
    3. Core C - Hydrophilic Low BET
    4. Core D - Hydrophilic High BET
b. Three desiccants:
    1. Desiccant A - Zeolite – Aluminosilicate 2mm in diameter, pore size 1nm.
    2. Desiccant B - activated CaO
    3. Desiccant C - granulate CaO

Description of the test procedure with the FS cores

The fumed silica core (300mm x300mm) was placed inside the bag of the system described above. The weight of the dry core was measured before it was placed inside the bag. Initial thermal conductivity was measured after a very long evacuation time. The temperatures of the plates of the LaserComp λ machine were set to 2°C and 18°C (10°C mean temperature). The part of the system containing the core material was kept for a few weeks between the plates of the λ machine for the entire duration of the test without changing the temperature setup. By doing so, the part of the system with the core was kept under a constant temperature gradient created by the different

temperatures of the plates. This ensured that the system was constantly very close to steady-state water distribution inside the core even when more water was inserted.

The leak-tight measuring glass tube filled with water was connected to the mVIP system and all the air molecules above the water level were removed by the turbo molecular pump. After opening the system valves, a slow delivery of water vapor from the glass tubing into the core area started, caused by the pressure difference between the core area and the water vapor pressure built inside the glass tubing due to evaporation. Very important: the temperature of the entire piping system was kept higher than the glass tubing to avoid internal condensation. Hot air was used for heating the piping system.

When the desired quantity of water was inserted the valves were closed and the panel was kept between the two plates of the λ machine to reach steady-state distribution of the water molecules inside the panel. By analyzing the changes of the λ readings we could see that constant λ values were measured after only a few hours. Presumably steady-state water concentration distribution inside the panel was achieved very quickly due to the slow delivery rate and especially because the slow process of increasing water content was carried out at a steady-state temperature gradient between the 2°C cold plate and the 18°C hot plate.

The same procedure of water injection was performed when the desiccants were analyzed; in this case the dry weight of desiccant was measured prior to the evacuation procedure. The thermal conductivity was not measured during the desiccant tests, only the pressure inside the system was continuously measured.

Results

Core A - Hydrophobic – dry weight – 283gr, density – 0.175 gr/cm^3

The graph and the table below describe the dependence of thermal conductivity as a function of water content at steady state conditions with 2°C on the cold side of the core material and 18°C on the warm side.

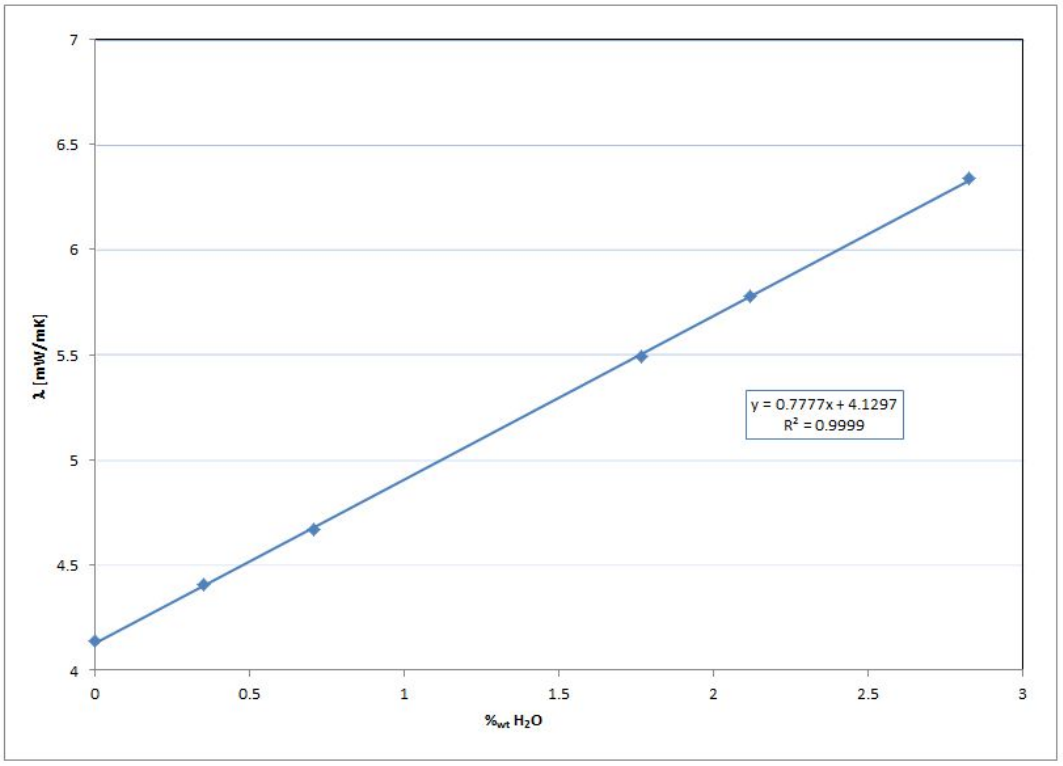

Figure 5: Thermal conductivity of Core A - Hydrophobic fumed silica as a function of water content.

Weight percentage of water	λ [mW/mK]
0	4.141
0.35	4.406
0.71	4.67
1.77	5.49
2.12	5.77
2.83	6.34

Table 1: Thermal conductivity of Core A - Hydrophobic fumed silica as a function of water content.

The set of results shows linear dependency of the thermal conductivity on the water content up to $3\%_{wt}$. A thermal conductivity increase rate of 0.7777 mW/mK per $\%_{wt}$ of H_2O is about 50% higher than the value of 0.5mW/mK per $\%_{wt}$ of H_2O measured by ZAE, which was adopted by the new CEN standard for VIPs in buildings. This observation tells us that different fumed silica grades can have very different responses to the adsorbed humidity. It also tells us that hydrophobic fumed silica is probably not the right choice to make.

Core B - Hydrophilic BET 200 g/m^2 – dry weight – 320gr, density – 0.175 gr/cm^3

The graph and the table below describe the dependence of thermal conductivity as a function of water content at steady state conditions with 2°C on the cold side of the core material and 18°C on the warm side.

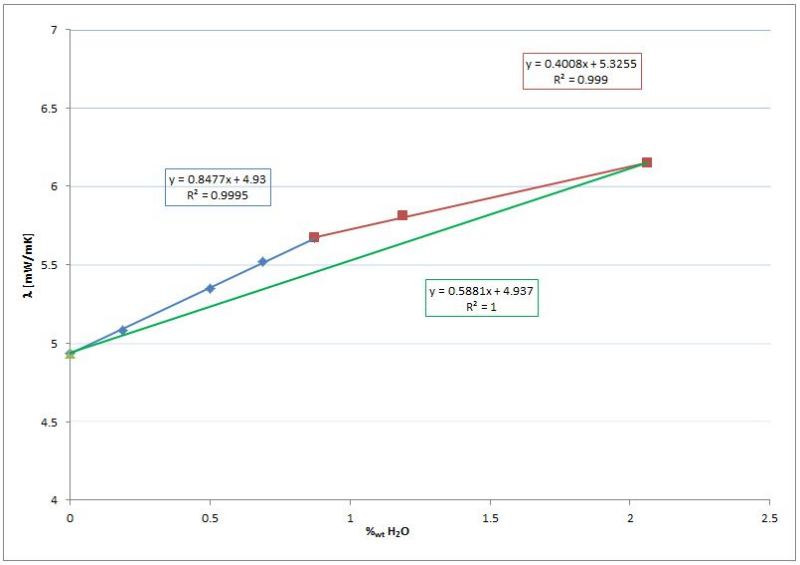

Figure 6: Thermal conductivity of Core B - Hydrophilic fumed silica as a function of water content.

Weight percentage of water	λ [mW/mK]
0	4.937
0.19	5.08
0.5	5.35
0.69	5.52
0.88	5.67
1.19	5.81
2.06	6.15

Table 2: Thermal conductivity of Core B - Hydrophilic fumed silica as a function of water content.

The set of results shows a relatively high thermal conductivity increase rate of 0.8477 mW/mK per %wt of H_2O up to about 0.8% WC which is higher than the CEN standard value by 60%. Adding more water into the system beyond 0.8% resulted in 2.1 times smaller thermal conductivity dependence on the water content. It is assumed that because of the temperature gradient inside the panel (2°C – 18°C) at about $1\%_{wt}$ water content, the dew point is reached at the internal cold side of the panel. In such a case the water partially condensates inside the panel, and partially desorbed from the fumed silica causing the dependency of thermal conductivity on the water content to decrease.

Core C - Hydrophilic low BET– dry weight – 323gr, density – 0.19 gr/cm^3

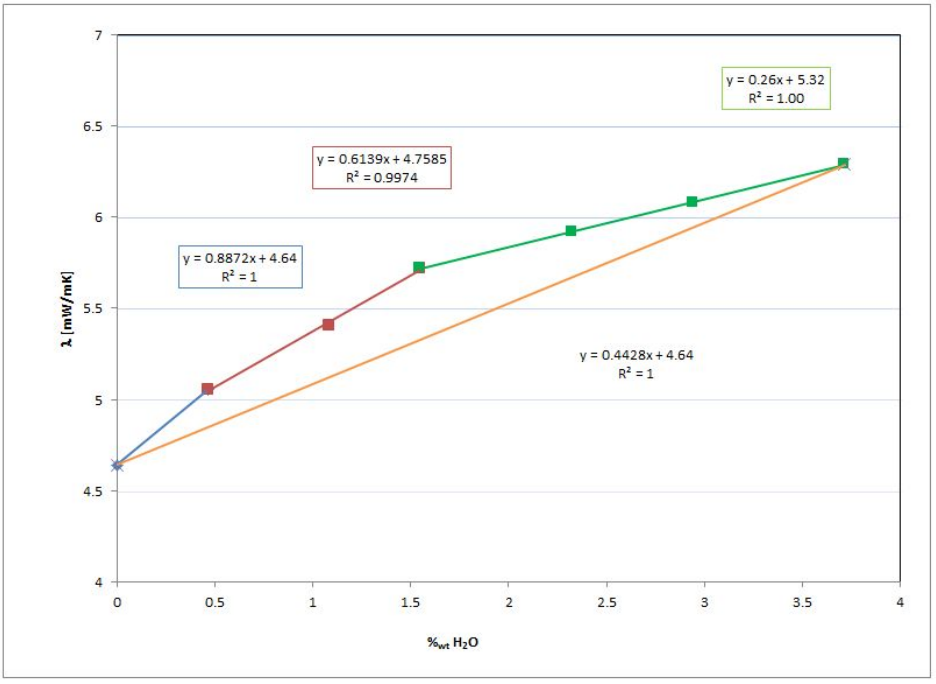

Figure 7: Thermal conductivity of Core C - Hydrophilic low BET fumed silica as a function of water content.

Weight percentage of water	λ [mW/mK]
0	4.64
0.46	5.052
1.08	5.404
1.55	5.72
2.32	5.92
2.94	6.08
3.72	6.285

Table 3: Thermal conductivity of Core C - Hydrophilic low BET fumed silica as a function of water content.

As in the previous samples, the increased rate of the thermal conductivity as a function of water content was found also to be dependent on the absolute value of the content of water. Up to 0.5%, the increase rate was quite high, almost double the value observed by ZEA. In the range of 0.5% to 1.5%, the increase was slightly higher than the commonly agreed upon value of 0.5mW/mK per 1% WC. At water content larger than 1.5%, the increase rate of the thermal conductivity was lower by a factor of 2 compared to the ZEA results. As before it is assumed that the decrease rate of the thermal conductivity as a function of water content was slowed down by partial condensation of water inside the system at higher levels of WC.

Core D - Hydrophilic high BET– dry weight – 330gr, density – 0.176 gr/cm^3

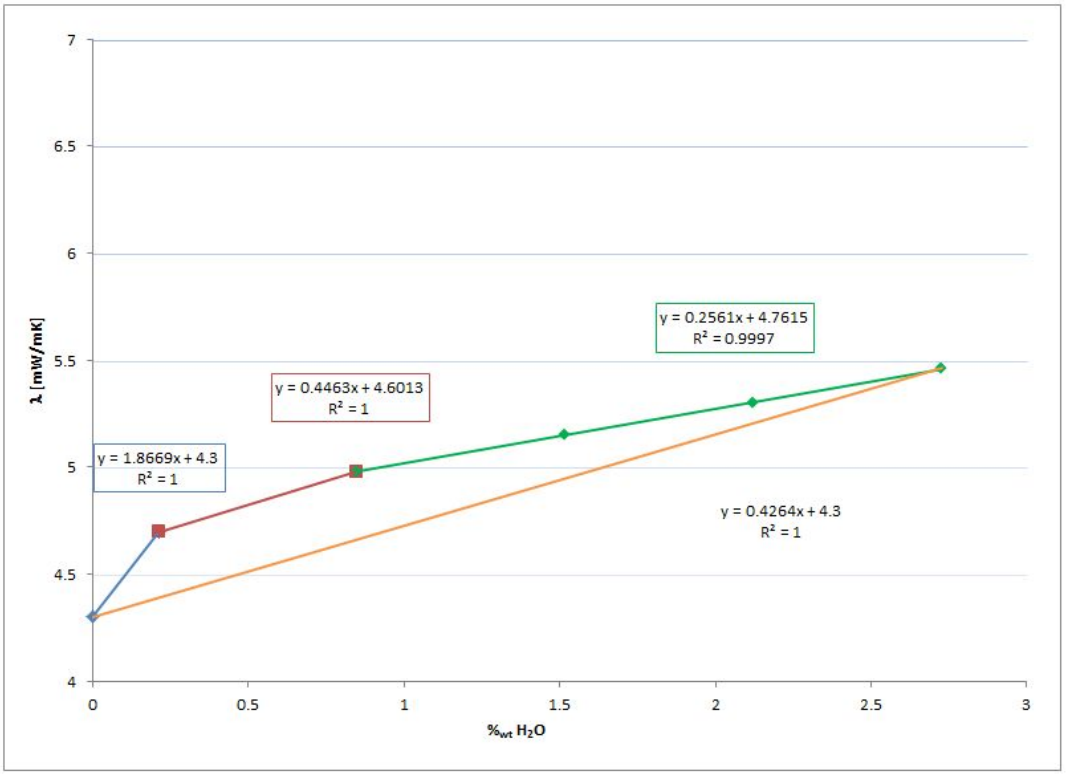

Figure 8: thermal conductivity of Core D - Hydrophilic high BET fumed silica as a function of water content.

Weight percentage of water	λ [mW/mK]
0	4.3
0.21	4.696
0.85	4.98
1.52	5.15
2.12	5.3
2.73	5.463

Table 4: Thermal conductivity of Core D - Hydrophilic low high fumed silica as a function of water content.

As in the two samples above, the increase rate of the thermal conductivity as a function of water content was very high at low levels of water content up to 0.2%, and dropped down rapidly below 0.5mW/mK per 1%WC. The last two samples received were from the same panel manufacturer and they had different surface area/g. Based on these test results one can assume that FS powders with higher surface area per gram will degrade more slowly due to moisture permeation than powders with smaller surface area. The dependence of the thermal conductivity on WC of all of the four FS grades tested and the ZAE results are shown in the graph below:

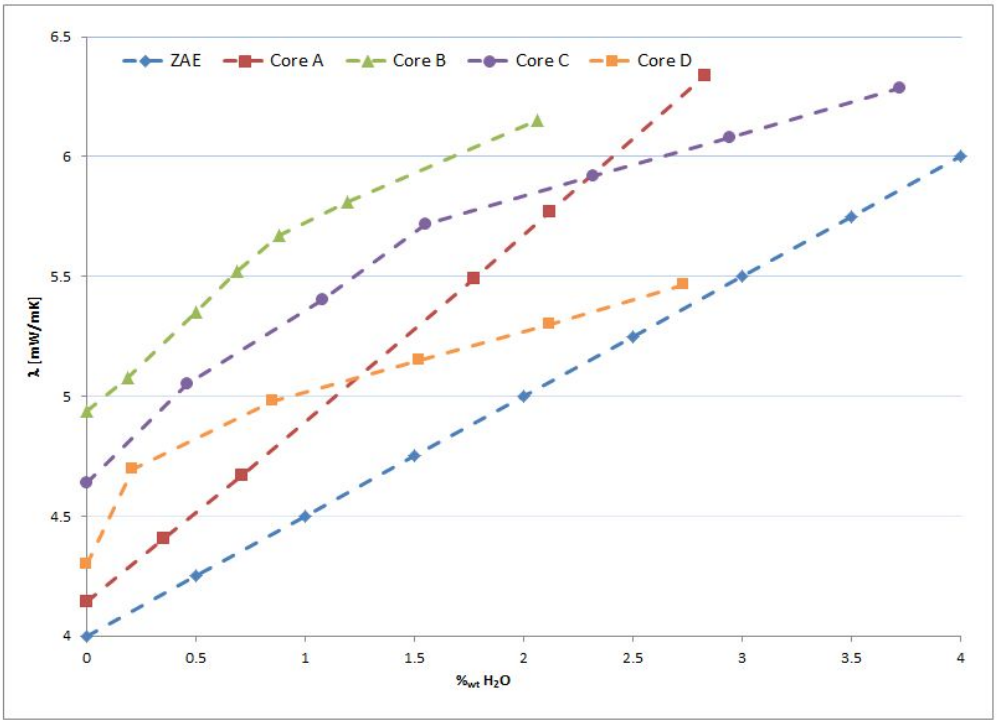

Figure 9: Thermal conductivity of different fumed silica cores as a function of water content.

The graph above tells us that different FS powders can have very different responses to the permeated water molecules, which, together with the differences in the initial thermal conductivity values, can have a substantial effect on the value of λ_D (The declared value of λ).

It is interesting to compare these new test results with the result of similar tests done on five FS cores in the previous VIPA funded project. See the graph below.

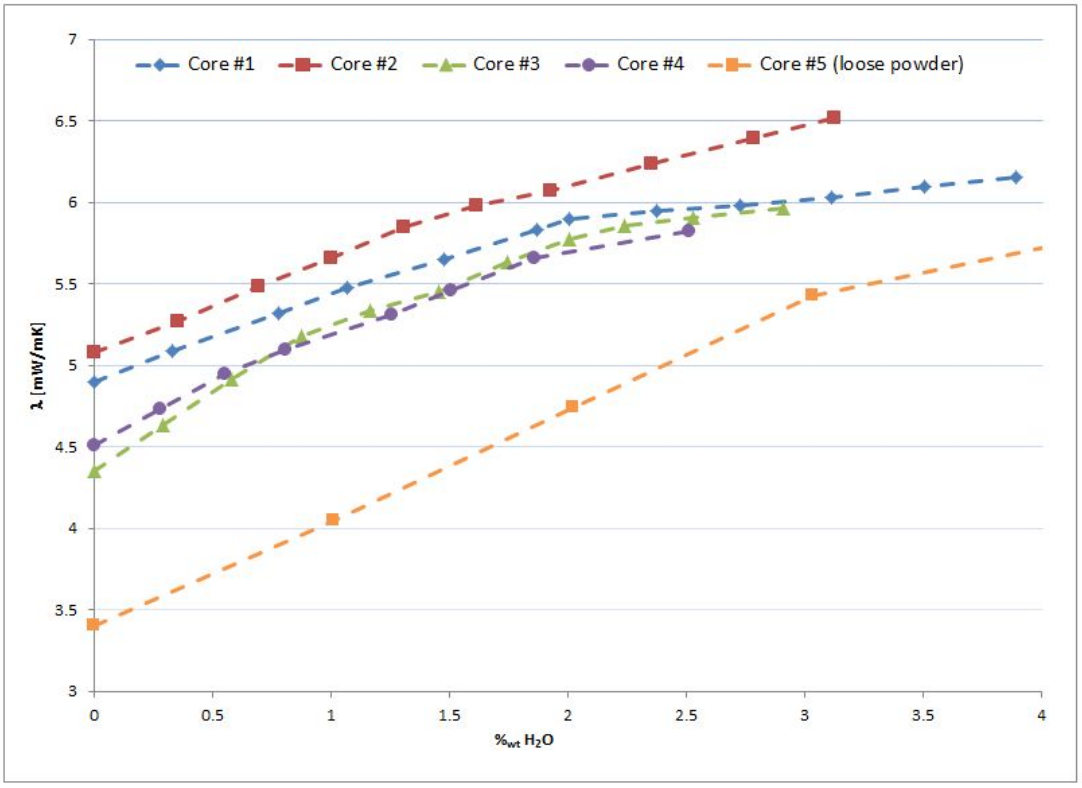

Figure 10: Thermal conductivity of different fumed silica cores as a function of water content.

Core #1		Core #2		Core #3		Core #4		Core #5	
%wt H_2O	Δ λ /% (mW/mK)/%	%wt H_2O	Δ λ /% (mW/mK)/%	%wt H_2O	Δ λ /% (mW/mK)/%	%wt H_2O	Δ λ /% (mW/mK)/%	%wt H_2O	Δ λ /% (mW/mK)/%
0 – 2	0.494	0 – 1.3	0.5915	0 – 0.9	0.9546	0 – 0.8	0.7395	0 - 3	0.6697
2 – 3.9	0.1327	1.3 – 3.1	0.3653	0.9 – 2.2	0.505	0.8 – 1.85	0.5288	3 – 6	0.3633
				2.2 – 2.9	0.1579	1.85 – 2.5	0.251		

Table 5: Increase rate of the thermal conductivity as a function of water content of different FS cores.

Testing the performance of desiccants

The goal of this test was to characterize the behavior of the desiccants (equilibrium water vapor pressure and capacity) as a function of the absorbed water weight percentage. We ran a similar preliminary study in the past.

Description of the old test: - The system with a water measuring tube was vacuum tightly connected to the bag of a fiberglass panel containing 10g of CaO desiccant. By opening the valve to the measuring tube, the desiccant drew measured amounts of water. After adding a known measured amount of water into the internal volume of the panel, the system was kept at room temperature and the water vapor pressure inside the panel was continuously measured after the pressure readings reached constant values (the equilibrium water vapor pressure at this specified % of absorbed water by the desiccant).

Table 5 and Figure 11 below describe the measured water vapor pressure as a function of the weight percentage of the water absorbed by the desiccant.

Water content (%)	Pressure (mbar)
10	0.365
15	0.56
20	0.71
28	0.96
38	2.6
45	above 10

Table 6: Water vapor pressure inside the panel at room temperature as function of the absorption percentage of water by the CaO desiccant.

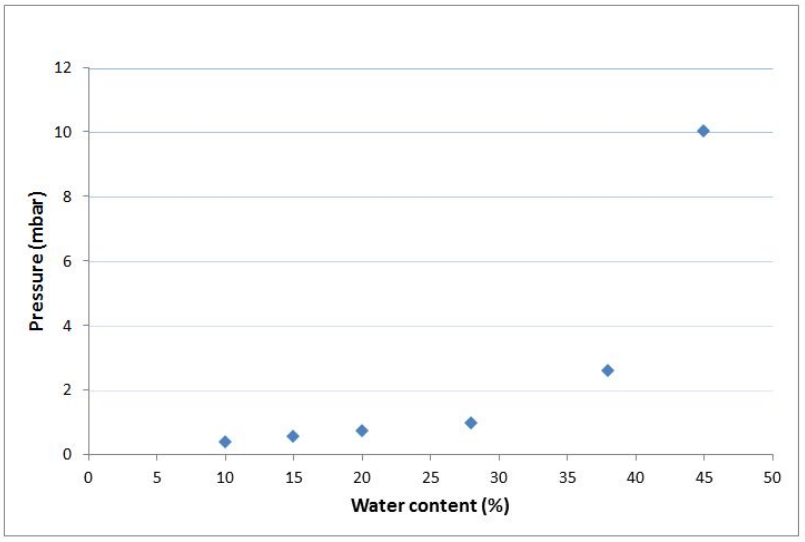

Figure 11: Water vapor pressure inside the system with CaO desiccant as function of the weight percentage of absorbed water.

These preliminary results support the common opinion that the absorption capacity of CaO desiccants is about 30% by weight when each calcium oxide molecule reacts with one water molecule creating one calcium hydroxide molecule. Above 32% absorption percentage, the desiccant is no longer active, causing fast moisture pressure buildup. The graph below shows the equilibrium moisture vapor pressure as a function of water content between 10% to 28%. Linear dependence of the pressure on the absorbed percentage was measured for this CaO desiccant at absorption levels smaller than 28%.

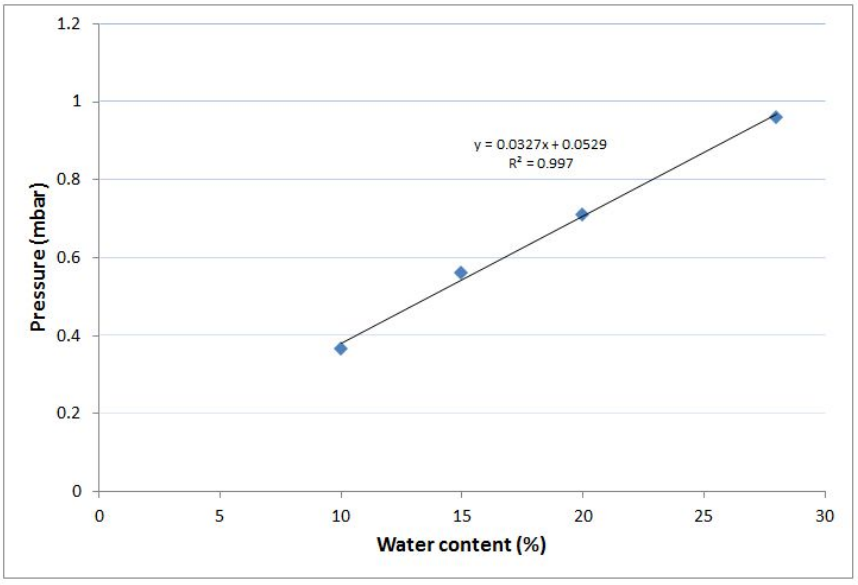

Figure 12: Water vapor pressure inside the system with CaO desiccant as function of the weight percentage (up to 28%) of absorbed water.

The figure above indicates that the water pressure increases by 0.0327 mbar per 1% of water content. Such an increase has an impact on the thermal conductivity of glass fiber panels, for core material with $P_{0.5}$ of 6.5mbar the increase rate of the thermal conductivity will be 0.116 (mW/mK)/%WC. At 20%WC the equilibrium water vapor pressure will increase the thermal conductivity of a fiber glass ($P_{0.5}$ = 7 mbar) panel by a very significant amount of 2.32 mW/mK.

Results of the new project

Desiccant A - Zeolite – Aluminosilicate pellets, 2mm in diameter. Pore size 1nm. (Physical adsorption)

The desiccant (24gr) was activated at 250°C for 3 hours prior to the system evacuation. To eliminate the effect of air permeation and air outgassing on the pressure reading the pressure increase rate of the system without water inside was measured prior to the water insertion.

Air pressure build up as function of time is presented in the figure below:

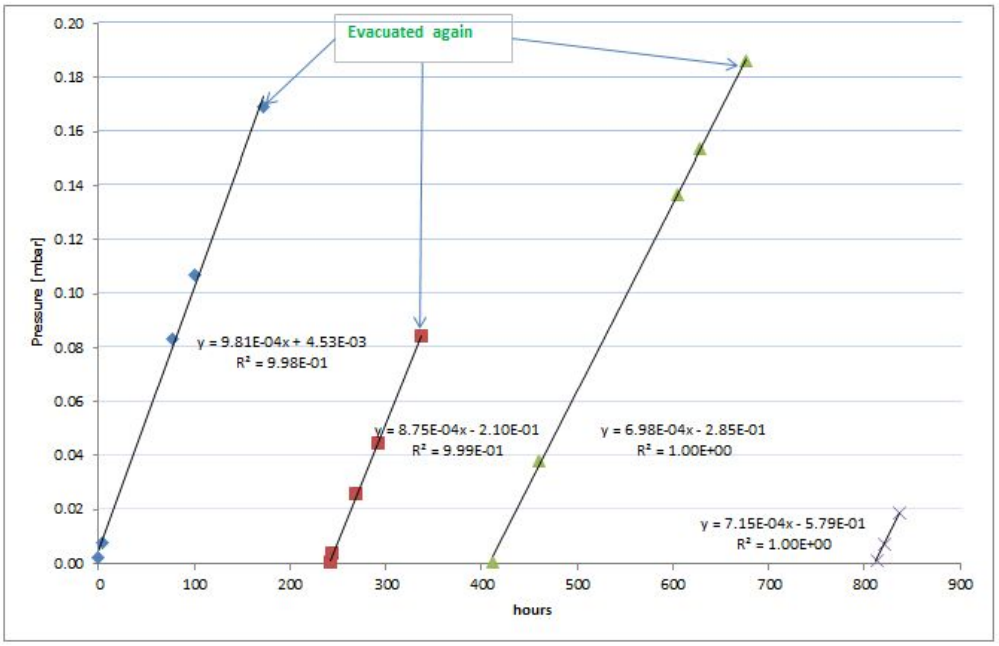

Figure 13: Pressure increase inside the system with desiccant A and without water.

The system was evacuated four times to insure no air outgassing during the test. The following figure presents the pressure inside the system with different water content of the Zeolite pellets. The small pressure increase rate due to air permeation (skin and side) only could be calculated from the slope of the curves in the graph above and could be used to calculate the net contribution of the actual moisture vapor pressure to the overall internal pressure inside the system.

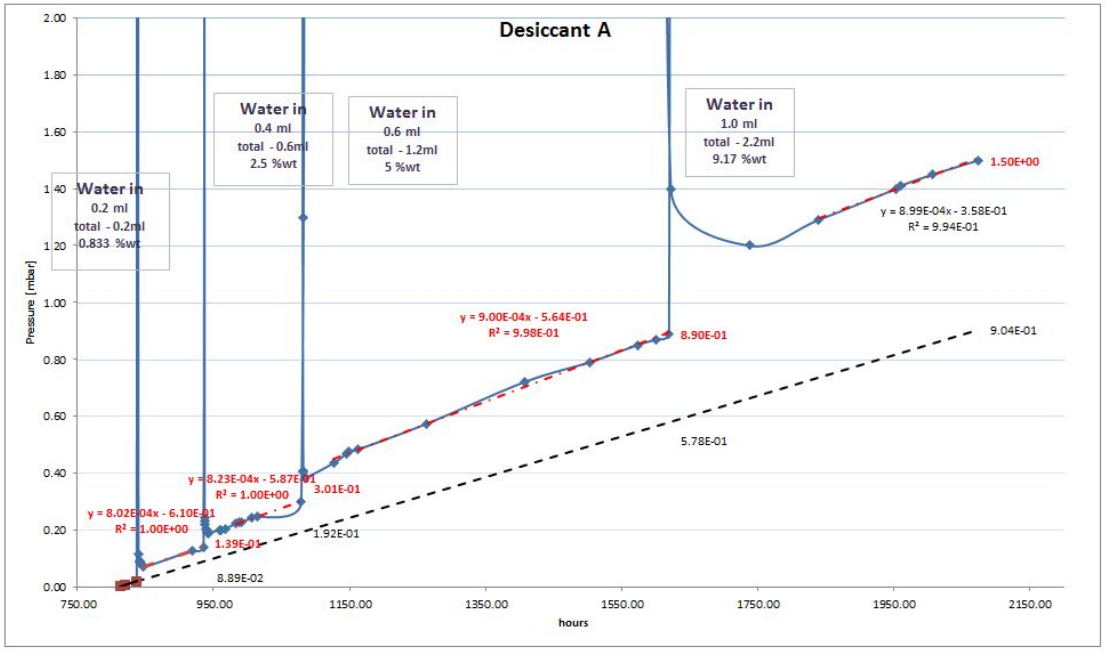

Figure 14: The pressure as a function of time and different content of water inside (% of the desiccant weight).

The blue line represents the readings of the overall pressure inside the panel containing the Zeolite desiccant. The sharp peaks represent the large jumps of moisture vapor pressure while the valve was open to allow extra moisture in. Right after closing the valve the pressure dropped down abruptly due to quick absorption by the desiccant. The black dashed line represents the expected air pressure inside the system due to the slow air permeation. The actual equilibrium water vapor pressure (total pressure minus the air pressure) as a function of the weight percent of the water absorbed by the zeolite pellets is presented in the table below:

Water content (%)	Pressure (mbar)
0.833	0.0501
2.5	0.109
5	0.312
9.17	0.596

Table 7: The equilibrium water vapor pressure at room temperature inside an FG panel containing desiccant A (Activated Zeolite) as function of the water absorption percentage.

As before, linear behavior was observed up to 9% adsorption by weight as shown in the graph below.

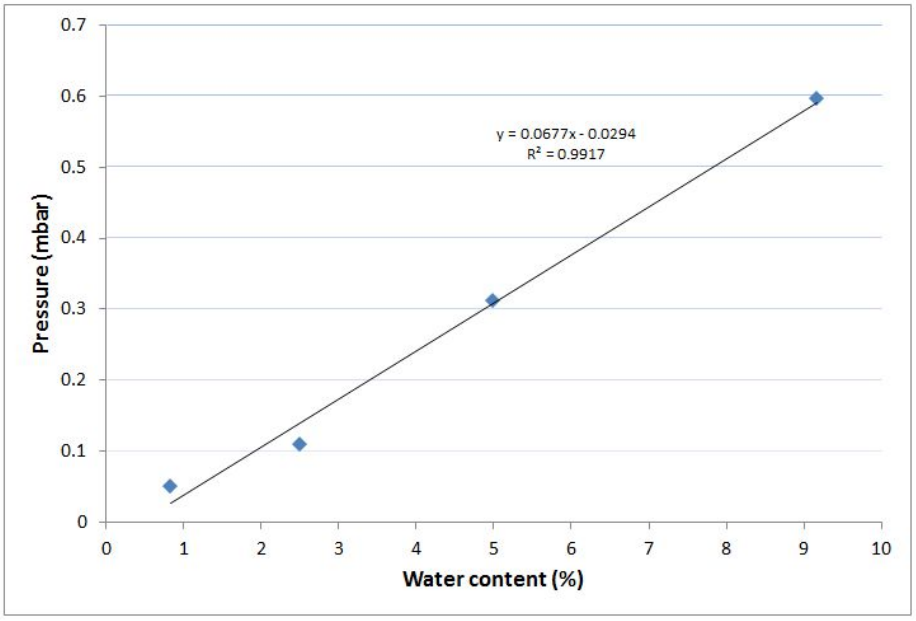

Figure 15: The equilibrium water vapor pressure inside the system with desiccant A (activated Zeolite) as a function of the weight percentage of the absorbed water. The pressure increase rate was found to be as large as 0.0677 mbar per 1% of absorbed water.

Desiccant B – activated CaO

Two bags of desiccant (10gr each) were placed inside a newly prepared system. As before, the pressure increase rate of the system without adding water in was determined prior to the water insertion. The internal air pressure as a function of time is presented in the figure below:

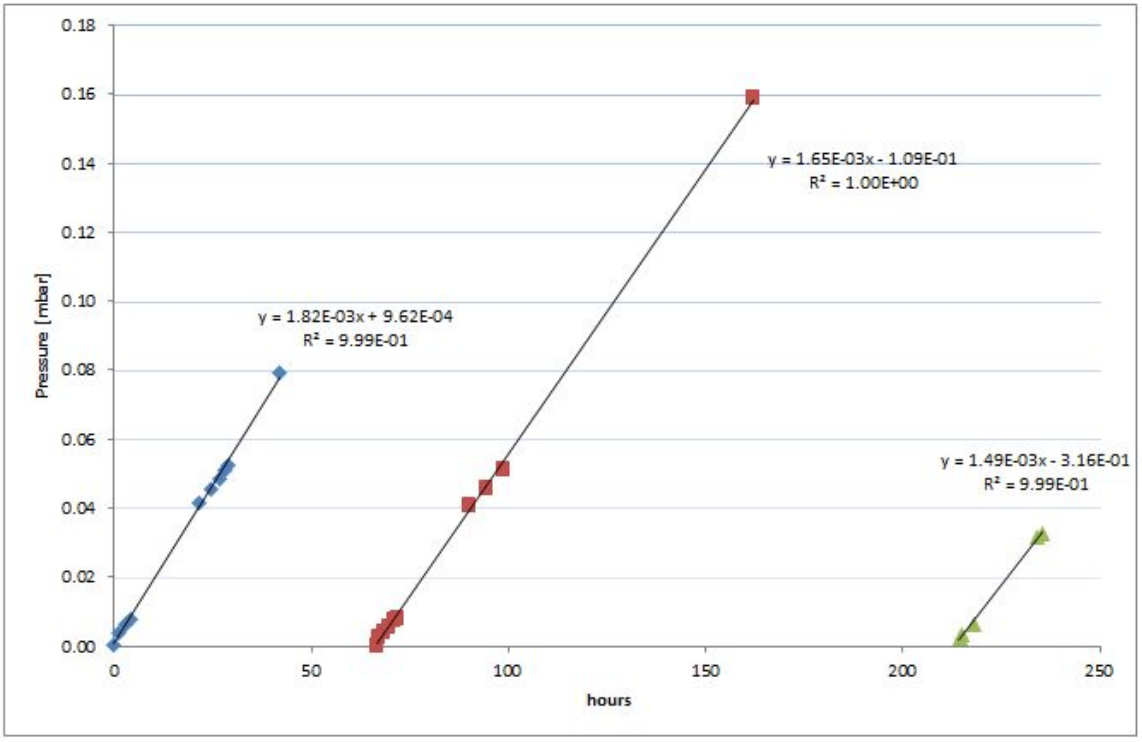

Figure 16: Pressure increase inside the system with desiccant B without water insertion. Evacuated three times.

The following figure presents the overall pressure inside the system at different water content levels.

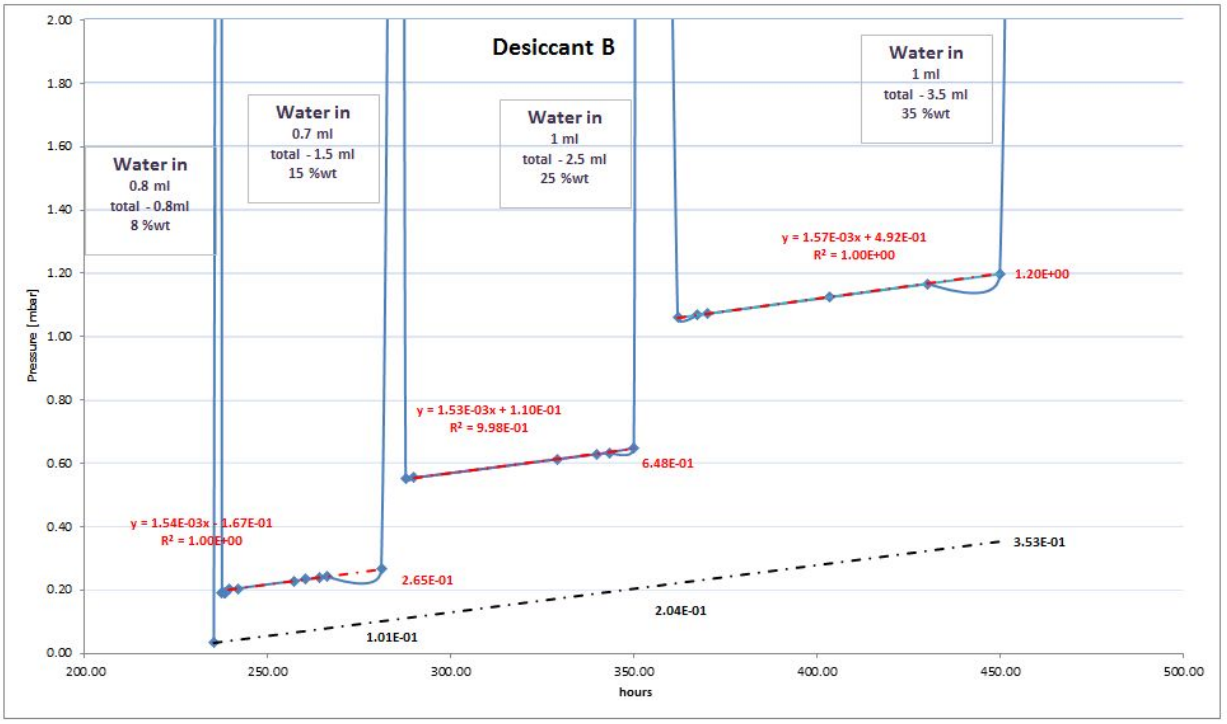

Figure 17: Desiccant B - pressure as a function of time with different content of water absorbed by the desiccant.

The equilibrium water vapor pressure (subtract of the absolute pressure and the expected air pressure due to permeation) as a function of the water content is presented in the table below:

Water content (%)	Pressure (mbar)
8	0.16
15	0.44
25	0.85
35	above 10

Table 8: Equilibrium water vapor pressure at room temperature inside the panel containing desiccant B as function of the absorption percentage.

As before linear behavior was observed up to water content of 25% as shown in the figure below.

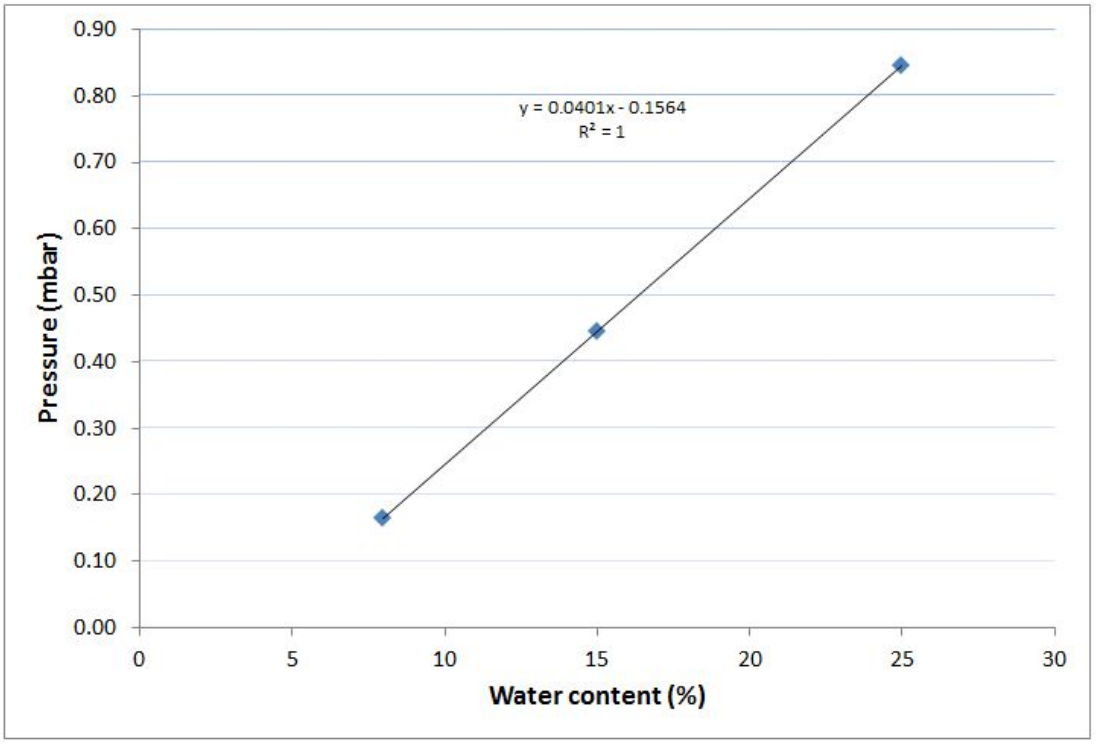

Figure 18: The equilibrium water vapor pressure inside the system with desiccant B (activated CaO) as function of the weight percentage of the absorbed water. Pressure increase is 0.04 mbar per 1% of water content

Desiccant C – granulate CaO

17.5 gr of desiccant (granulate CaO) were placed inside the newly prepared system. As before the pressure increase rate of the system without water inside was determined prior to the water insertion. The internal air pressure as a function of time is presented in the figure below:

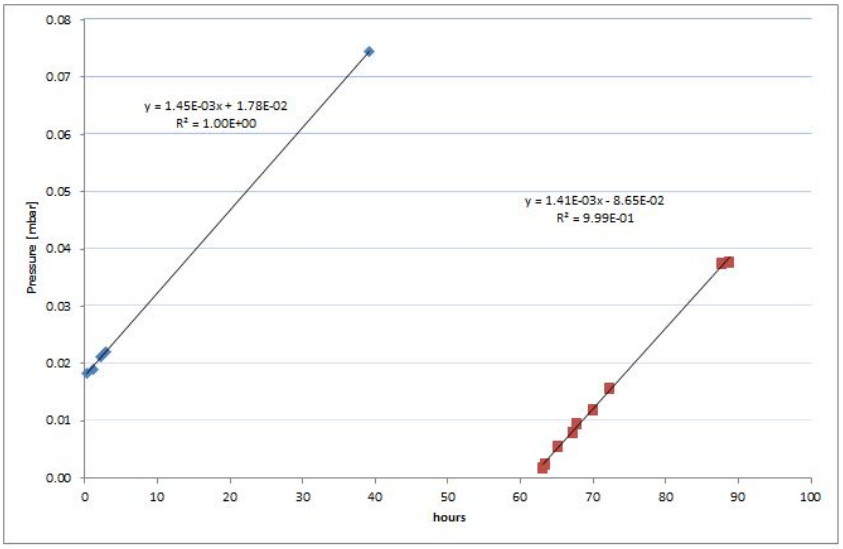

Figure 19: The pressure increase rate inside the system with desiccant C due to air permeation only. Two evacuations.

The following figure presents the overall pressure inside the system with different water content levels.

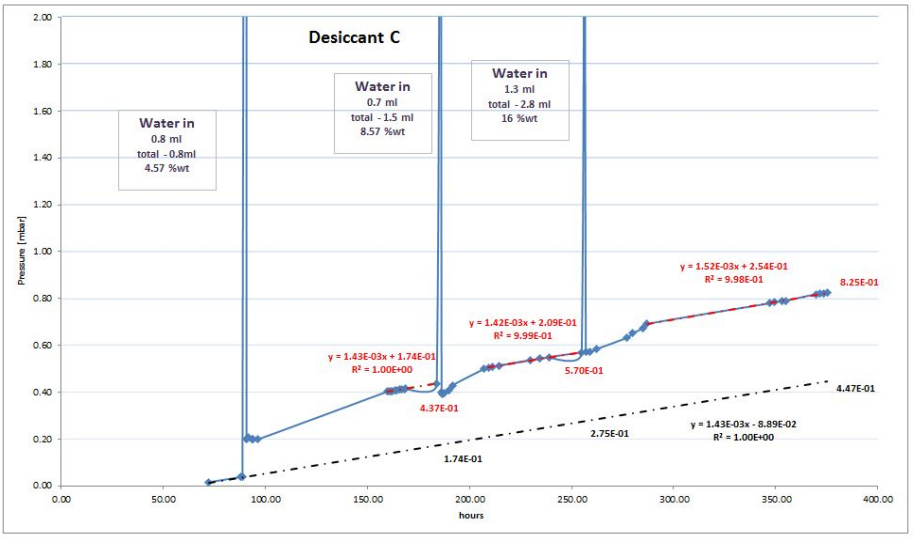

Figure 20: Water vapor pressure inside the system with desiccant C as function of the weight percentage of absorbed water.

As before, linear behavior was observed far from saturation as shown in the figure below.

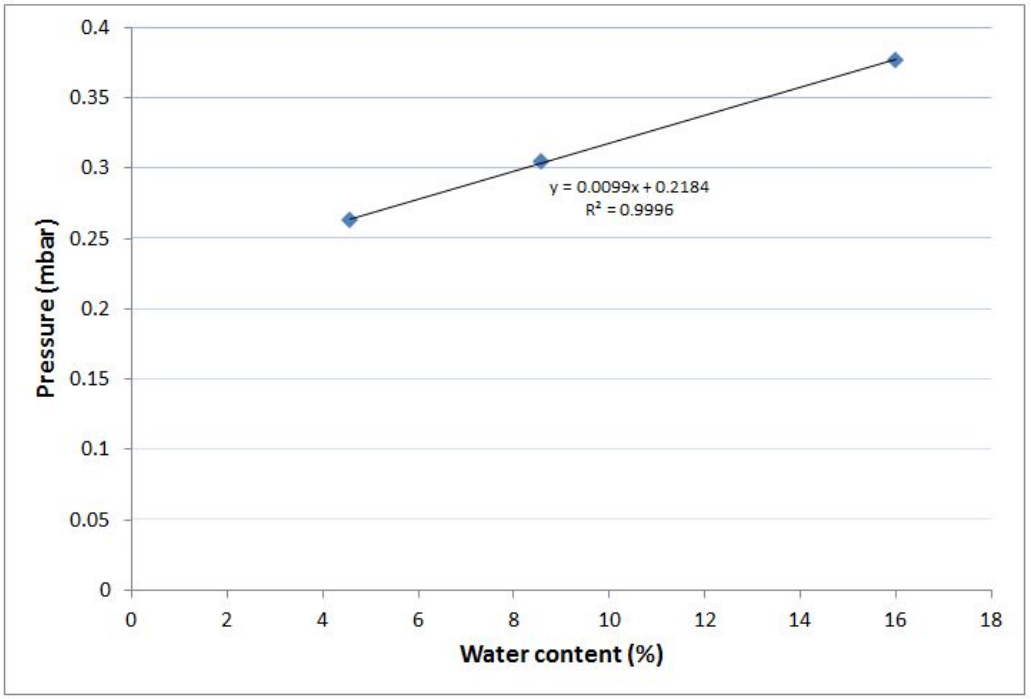

Figure 21: The equilibrium water vapor pressure inside the system with desiccant C (granulate CaO) as function of the weight percentage of the absorbed water. Pressure increase rate of 0.01 mbar per 1% of water content percent (very small) was measured.

The equilibrium water vapor pressure (subtract of absolute and expected air pressure) as a function of the water content is presented also in the table below:

Water content (%)	Pressure (mbar)
4.57	0.263
8.57	0.305
16	.377

Table 9: The equilibrium water vapor pressure at room temperature of desiccant C (granulate CaO) as function of the water absorption percentage.

The figure below shows the equilibrium water vapor pressure inside the panels as a function of the percentage of water absorbed by the three types of desiccants tested.

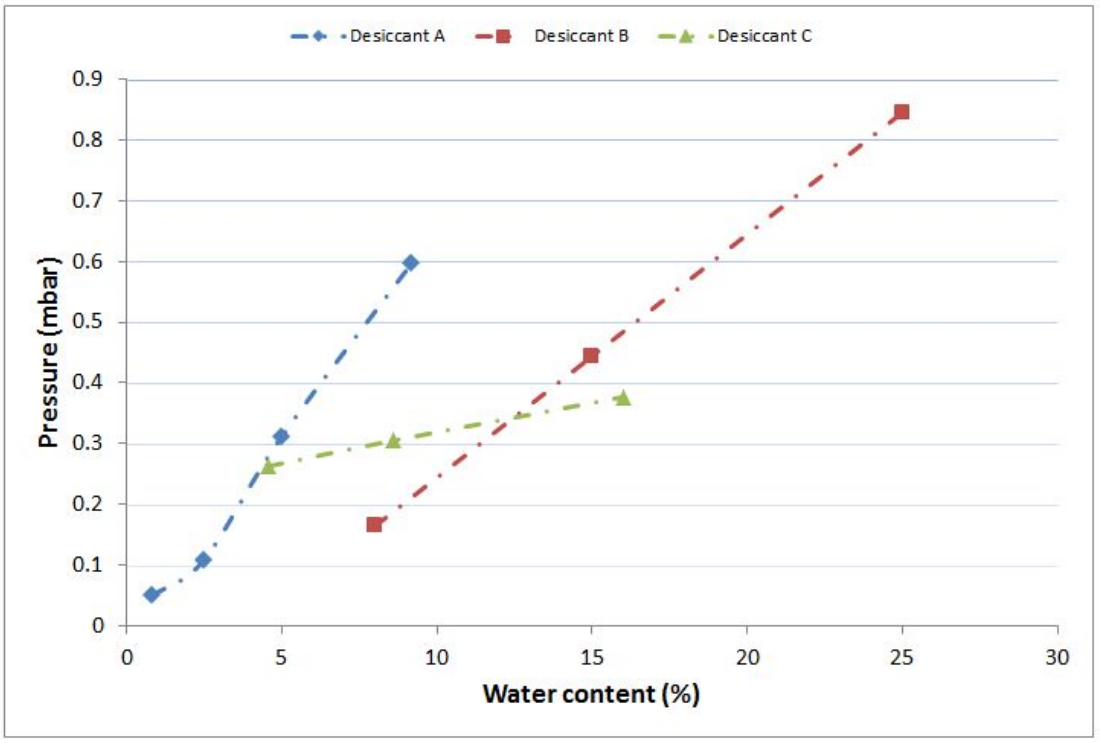

Figure 22: The equilibrium water vapor pressure inside the system with different desiccants far from saturation as a function of the weight percentage of the absorbed water.

The results point out that each desiccant has its own unique behavior as a function of the percentage of absorbed water. It is easy to see that desiccant A (activated zeolite) absorbs less efficiently the water molecules than the Cao desiccants, causing relatively large equilibrium water pressure. For FG panels this water pressure build up may cause a larger than expected increase of the thermal conductivity even at a relatively low percentage of water adsorption by the zeolite powder. Another very interesting result is the difference between desiccant B (activated CaO) and desiccant C (granulate CaO): The equilibrium water pressure buildup rate with granulate CaO was found to be four times smaller than that of activated CaO, and almost seven times smaller than with activated zeolite.

The marked effect of the measured equilibrium water vapor pressure on the thermal conductivity of FG panels is presented in the table below, where the extra contribution of the water pressure to the thermal conductivity of FG panels with $P_{1/2}$=7mbar was calculated for four absorption percentage levels.

	$\Delta\ \lambda$ [mW/mK]		
Water content	Desiccant A	Desiccant B	Desiccant C
1	0.239	0.142	0.036
5	1.195	0.71	0.18
10	2.39	1.42	0.36
15	3.585	2.13	0.54

Table 10: Expected thermal conductivity increase due to the water pressure of fiberglass ($P_{0.5}$=7mbar) panel as a function of the water absorption percentage for the three tested desiccant types.

Conclusions

Tests made on the FS cores:

- A very accurate and easy to operate technique was developed for measuring the dependency of thermal conductivity of fumed silica cores on absorbed water content. This technique, based on the λ vs P technology, is very inexpensive and can easily be adopted by any research or industrial laboratory. The only drawback of the technique is the time taken to reach steady state for each data point. In some cases it was up to a week.

- Four different fumed silica cores were analyzed; it was found that each had a very different dependence of its thermal conductivity on water content inside.

- For three out of four fumed silica cores the slope $d\lambda/d\%_{wt}H_2O$ was much steeper at low levels of water content, and more moderate at higher levels of water content. The initial slopes and the turning points slopes were different for each of the three cores.

- In view of the results of this research, it is worth reviewing the assumption made in the CEN and the ISO standards documents for VIPs in building that all fumed silica cores respond identically to the percent of moisture content.

Tests made with the desiccants:

- An important outcome of the project was the development of an accurate technique for determining the equilibrium water pressure of desiccants as a function of the percentage of absorbed water. This is an inexpensive system that can easily be adopted by any industrial or research lab.

- The three different types of desiccants were found to have very different dependence of the equilibrium water vapor pressure on the water absorbed percentage. The newly developed testing technique can also help to make the optimal decision on what type of desiccant to use with fiberglass panels and panels cores having small $P_{1/2}$ values.

- The technique developed in this research provides a very efficient tool to better predict the lifetime performance of panels containing desiccants, and also can help to achieve more accurate values for λ declared for such panels. It is therefore recommended that this new testing technique will be adopted by the different VIP standards.

Signed:

Eddie Shufer and Dr. Yoash Carmi
Avery Dennison Hanita

November 5, 2020

References

1. Schwab H. Heinemann U. Beck A. Ebert H-P. Fricke J. J. Thermal Environ. Bldg. Sci. 2005, 28, 293-317